An AFM Study of the Deformation and Nanorheology of Cross-Linked PDMS Droplets

ARTICLE *in* LANGMUIR · MARCH 2002

Impact Factor: 4.46 · DOI: 10.1021/la011461g

3 AUTHORS, INCLUDING:

Clive A Prestidge
University of South Australia
168 PUBLICATIONS **3,166** CITATIONS

An AFM Study of the Deformation and Nanorheology of Cross-Linked PDMS Droplets

Graeme Gillies, Clive A. Prestidge, and Phil Attard*

Ian Wark Research Institute, University of South Australia, Mawson Lakes, South Australia 5095, Australia

Received September 21, 2001. In Final Form: November 16, 2001

Interaction forces between a spherical silica probe and a cross-linked poly(dimethylsiloxane) (PDMS) colloidal droplet have been determined by atomic force microscopy (AFM). On approach of the surfaces, as a result of deformation of the PDMS, the repulsive force increases much less rapidly than expected for electrical double layer interaction of rigid particles. The amount of deformation is dependent on the loading force and the drive velocity and reflects the nanorheological response of the PDMS. On retraction of the surfaces, force curve hysteresis is observed and is dependent on the rate of approach/retraction. Hysteresis is due to the viscoelastic response of the PDMS droplet and can be described by theory (Attard, P. *Phys. Rev. E* **2001**, *63*, 061604). The moduli and the characteristic relaxation time of the PDMS colloid have been determined from the force measurements and offer a novel description of the nanorheological properties.

Introduction

Interaction forces between colloidal particles have been extensively investigated using the atomic force microscope (AFM) in colloid probe mode.[1−14] Electrostatic,[1,2] hydration,[2] van der Waals[3], steric,[4,5] and hydrophobic forces,[6,7] as well as forces introduced due to both adsorbing[8] and nonadsorbing[9] polymer molecules, have been determined. Furthermore, strong correlation between the measured interaction forces and colloid stability,[5] particle adhesion,[5,7] and suspension rheology[5,7] have been reported. These studies have mainly focused on nondeformable colloids, but in recent times, with the increased desire to understand the interaction and stability of bubbles in foams and froths, droplets in emulsions, and deformable biological macrostructures and cells, attention has moved to AFM studies on deformable systems.[8,10−14] Colloid probe AFM studies on bubbles[10,11] oil droplets,[8,12] and polymer colloids[13,14] have all been reported. However, a fully quantitative description of the interplay between deformation and interaction has yet to be applied to measured data.

Upon interaction of a deformable colloid with either another colloidal particle or a surface, deformation results in additional variation of the surface separation and/or the contact area, and it is inappropriate to describe the interaction behavior in the same way as for rigid colloids.[1−4] Deformation and interaction of macroscopic surfaces has also received considerable interest of late. For example, the shape of a mercury drop has been obtained using the surface forces apparatus (SFA).[15] Young's modulus and the surface energy of soft lenses or substrates have been determined using the Johnson, Kendall, and Roberts (JKR) apparatus by fitting the contact area, adhesion, and the deformation to elastic JKR theory.[16] In addition the deformation and elastic vibration of glass lenses have been measured using the measurement and analysis of surface and interaction forces (MASIF) apparatus.[17]

In considering colloid probe AFM studies on deformable systems, there are two major difficulties:

(i) There is no sharp transition between contact and noncontact, because deformation occurs prior to contact due to the extended range of surface forces. Therefore, the zero of separation cannot be determined in the same way as for rigid bodies.

(ii) The increasing deformation of the colloid with load means that even when in contact the cantilever does not move the drive distance. Although the compliance may appear linear at high loads, this should not be mistaken for rigid substrate compliance since deformation is still occurring. Thus, the resultant slope in this region should not be used to calibrate the photodiode.

Any quantitative AFM force measurement should address both issues. We have shown that because deformation is negligible for weak forces, the zero of separation can be established by shifting the data to coincide with the known rigid body interaction at large separations where forces are weak.[18] In this instance we used known surface potentials to calculate nominal separation on the basis of the renormalized linear Poisson−Boltzmann

* To whom correspondence may be addressed. E-mail: phil.attard@unisa.edu.au.

(1) Butt, H.-J. *Biophys. J.* **1991**, *60*, 777.
(2) Ducker, W. A.; Senden, T. J.; Pashley, R. M. *Nature* 1991, *353*, 239.
(3) Hartmann, U. *Phys. Rev. B* 1991, *43*, 2404.
(4) Butt, H.-J.; Kappl, M.; Mueller, H.; Raiteri, R. *Langmuir* **1999**, *15*, 2559.
(5) Addai-Mensah, J.; Dawe, J.; Hayes, R. A.; Prestidge, C. A.; Ralston, J. *J. Colloid Interface Sci.* **1998**, *203*, 115.
(6) Carambassis, A.; Jonker, L. C.; Attard, P.; Rutland, M. W. *Phys. Rev. Lett.* **1998**, *80*, 5357.
(7) Muster, T. H.; Toikka, G.; Hayes, R. A.; Prestidge, C. A.; Ralston, J. *Colloids Surf., A* **1996**, *106*, 203.
(8) Hartley, P. G.; Grieser, F.; Mulvaney, P.; Stevens, G. W. *Langmuir* **1999**, *15*, 7882.
(9) Milling, A.; Biggs, S. R. *J. Colloid Interface Sci.* **1995**, *170*, 604.
(10) Ducker, W. A.; Zhenghe, X.; Israelachvili, J. N. *Langmuir* **1994**, *10*, 3279.
(11) Fielden, M. L.; Hayes, R. A.; Ralston, J. *Langmuir* **1996**, *12*, 3721.
(12) Aston, D. E.; Berg, J. C. *J. Colloid Interface Sci.* **2001**, *235*, 162.
(13) Vakarelski, I. U.; Toritani, A.; Nakayama, M.; Higashitani, K. *Langmuir* **2001**, *17*, 4739.
(14) Biggs, S.; Spinks, G. *J. Adhes. Sci. Technol.* **1998**, *12*, 461.
(15) Connor, J. N.; Horn, R. G.; Miklavcic, S. *Uzbek J. Phys.* **1999**, *1*, 99.
(16) Deruelle, M.; Hervet, H.; Jandeau, G.; Léger, L. *J. Adhes. Sci. Technol.* **1998**, *2*, 225.
(17) Attard, P.; Schulz, J.; Rutland, M. W. *Rev. Sci. Instrum.* **1998**, *69*, 3852.
(18) Gillies, G.; Prestidge, C. A.; Attard, P. *Langmuir* **2001**, *17*, 7955.

10.1021/la011461g CCC: $22.00
Published on Web 02/08/2002

equation. One way to calibrate the photodiode is to press against a hard surface prior to measuring the deformable object, which we do here.

In this study, we have performed AFM force studies on deformable poly(dimethylsiloxane) (PDMS) colloids. Here we focus on highly cross-linked PDMS droplets with Young's moduli in the range 10^6 N m^{-2}. A particular feature of the PDMS system under investigation is that altering the amount of cross-linking can control the deformability.[19] Complementary studies on more "liquidlike" droplets will be reported separately. The colloidal bodies studied here are viscoelastic rather than elastic in nature, and we pay particular attention to time-dependent, i.e., dynamic, deformation effects. Force data are analyzed using a relatively sophisticated theory[20] for the interaction of viscoelastic particles that takes into account the extended range of the surface force.

Theory

Elasticity. Traditionally the deformation of elastic particles has been described by Hertz[21] and JKR[22] theories. In particular Hertz theory has been used to predict the contact area as a function of the applied load, while JKR theory has been used to relate the adhesion to the surface energy. Both approaches assume particles only interact when in contact and ignore the extended range of the interactions in real systems. For example the electric double layer force can have a measurable range of 50−100 nm and the van der Waals attraction can be measured at 5−10 nm separation. Beyond Hertz and JKR contact theories are the soft contact approaches,[23−26] which take into account these extended interactions. Like Hertz and JKR theory they are based on linear elasticity. However, the contact theories assume particular analytic expressions for the pressure profile, namely those necessary to give a flat contact region. In contrast the soft contact theories calculate the pressure profile, local separation, and deformation self-consistently using the prescribed force law.

In soft contact theory the pressure profile $p(s)$ is related to the given formulas for the pressure between flat surfaces $p_\infty(h)$ separated by h by

$$p(s) = p_\infty(h(s)) \tag{1}$$

The local separation between the surfaces at a distance s from the axis is given by

$$h(s) = h_0(s) - U(s) \tag{2}$$

where $h_0(s)$ is the local separation between the undeformed surfaces. Finally the local deformation $U(r)$ is given by

$$U(r) = \frac{-2}{\pi E}\int d\mathbf{s}\,\frac{p(s)}{|\mathbf{r}-\mathbf{s}|} \tag{3}$$

Here the elasticity parameter is related to Young's modulus (E) and Poisson's ratio (ν) of each material by $2/E = (1-\nu_1^2)/E_1 + (1-\nu_2^2)/E_2$. This expression assumes that the two interacting particles are circularly symmetric. These three equations are solved by iteration to self-consistency.[25−27]

At this point is important to distinguish between the actual separation h and the nominal separation h_0. The nominal separation is the separation between two bodies if no deformation had taken place, whereas the actual separation is the actual distance between these bodies.

Viscoelasticity. An analogous soft contact theory has recently been developed for viscoelastic systems.[20,28] Time dependence is introduced into the above by including the rate of change of applied pressure,

$$U(r,t) - U(r,t_0) = \int_{t_0}^{t} dt'\,\frac{-2}{\pi E(t-t')}\int d\mathbf{s}\,\frac{\dot{p}_\infty(h(s,t'))}{|\mathbf{r}-\mathbf{s}|} \tag{4}$$

Here $\dot{p}_\infty(h(r,t)) = p'_\infty(h(r,t))\dot{h}(r,t)$ is the time rate of change of the pressure, $\dot{h}(r,t)$ is the time rate of change of local separation, and $E(t)$ is the time-dependent elasticity parameter (its reciprocal is often called the creep compliance function).

Viscoelastic materials are initially hard and soften or relax over time. The simplest material is characterized by two elastic limits representing short term, E_0, and long term, E_∞, behavior as well as a characteristic relaxation time τ,

$$\frac{1}{E(t)} = \frac{1}{E_\infty} + \frac{E_\infty - E_0}{E_0 E_\infty}e^{-t/\tau} \tag{5}$$

With this model, the deformation eq 4 can be transformed into a differential equation that can be solved by simple time stepping for any specified trajectory $h_0(t)$.

Electrical Double-Layer Pressure. In the results presented below we have used an electric double layer force law,

$$p(h) = p_0 e^{-\kappa h} \tag{6}$$

where

$$p_0 = 2\epsilon_r\epsilon_0\kappa^2\left(\frac{4k_BT}{ze}\right)^2\gamma^2 \tag{7a}$$

and

$$\gamma = \tanh\frac{ze\psi}{4k_BT} \tag{7b}$$

Here ϵ_r is the dielectric constant of water, ϵ_0 is the permittivity of free space, κ^{-1} is the Debye length, k_B is Boltzmann's constant, T is the absolute temperature, z is the valency of the electrolyte, and e is the charge of an electron.

This is derived from the linear Poisson−Boltzmann theory. The surface potentials ψ have been renormalized to give the same pressure as the nonlinear Poisson−Boltzmann theory at large separations. Typically $p_0 = 4.0 \times 10^4$ N m^{-2} and the decay length $\kappa^{-1} = 9.6$ nm.

Steric Pressure. Short-ranged steric forces are also expected to be present. For example, such a force has been measured between cantilever tips and grafted polymers on a silicon and aluminum oxide surfaces.[4] Likewise the surface of the PDMS spheres is expected to comprise a "hairy layer" in which case the steric pressure may be approximated by

$$p(h) = p_h e^{-h/\lambda} \tag{8}$$

Values of $p_h = 1.0 \times 10^{-8}$ N m^{-2} and the decay length of $\lambda = 1.5 \times 10^{-9}$ have been fitted below.

Materials and Methods

Preparation and Manipulation of PDMS Droplets. Emulsions of PDMS droplets in water were prepared through the base-catalyzed polymerization of diethoxydimethylsilane (DEDMS) and triethoxymethylsilane (TEMS) using a modified version of the method reported by Obey et al.[29] (DEDMS and TEMS were supplied by Aldrich, Milwaukee, WI, and distilled prior to use). An aqueous solution containing 1% (by volume) DEDMS, 1% TEMS, and 9% ammonia was sealed in a 250-mL reaction vessel, vigorously shaken for 30 s, and then placed on

(19) Barnes, T.; Prestidge, C. A. *Langmuir* **2000**, *16*, 4116.
(20) Attard, P. *Phys. Rev. E* **2001**, *63*, 061604.
(21) Hertz, H.; Reine, J. *Angew. Math.* **1881**, *92*, 156.
(22) Johnson, K. L.; Kendall, K.; Roberts, A. D. *Proc. R. Soc. London, Ser. A* **1971**, *324*, 301.
(23) Hughes, B. D.; White, L. R. *Quart. J. Mech. Appl. Math.* **1979**, *32*, 445.
(24) Muller, V. M.; Yushchenko, V. S.; Derjaguin, B. V. *J. Colloid Interface Sci.* **1980**, *77*, 91.
(25) Attard, P.; Parker, J. L. *Phys. Rev. A* **1992**, *46*, 7959.
(26) Attard, P. *J. Phys. Chem. B* **2000**, *104*, 10635.
(27) Attard, P. *Phys. Rev. E* **2001**, *63*, 011601.
(28) Attard, P. *Langmuir* **2001**, *17*, 4322.
(29) Obey, T. M.; Vincent, B. *J. Colloid Interface Sci.* **1994**, *163*, 454.

a rotating frame for 5 h. The polymerization was then quenched by dialysis against Milli-Q water for 24 h. The PDMS emulsion droplets that formed were highly monodisperse, with an average diameter of 600 nm, as determined by dynamic light scattering (Brookhaven Instruments). The dilute emulsion was left in contact with a 12 mm glass disk (Menzel-Glaser) for 3 days, in which time the PDMS droplets adhered to the glass surface. (The glass disk was preconditioned by washing in *n*-heptane, ethanol, 5 M KOH solution, and Milli-Q water and then treated with a water-plasma for 5 min). Excess PDMS droplets were washed off, and the glass disk was stored in aqueous solution prior to AFM analysis.

Atomic Force Microscopy. A Nanoscope III atomic force microscope (Digital Instruments, Santa Barbara, CA) was used to locate a PDMS droplet on the glass substrate and to measure the forces of interaction between an isolated PDMS droplet and a silica probe. Prior to mounting the colloid probe, the spring constant of the AFM cantilever was characterized using the method described by Cleeveland et al.[30] Silica spheres (radius 3.5 μm, Geltech, Alachua, FL) were manipulated using a thin tungsten wire and attached to the apex of AFM cantilevers with molten Shell Epikote 1004 resin.[31] Immobilized PDMS droplets were located in image mode, with the colloid probe attached to the cantilever; and then the in-built software was used to center the PDMS droplet directly beneath the colloid probe. The AFM was then operated in force mode, and single approach/retraction force versus distance measurements were determined at particular drive velocities (0.06−4 μm/s) and maximum loading forces of up to 30 nN. To quantify the force data the AFM photodiode was calibrated from the constant compliance region of force curves between the silica probe and the glass substrate in a region free from immobilized PDMS droplets. The force (F) acting between the silica probe and PDMS droplet was determined from the cantilevers deflection using Hooke's Law, $F = kD$, where k represents the spring constant and D the deflection of the cantilever. All force versus distance measurements where determined at pH 9.3 in the presence of a 10^{-3} M KNO_3 background electrolyte; the corresponding ζ potentials[19] for the PDMS droplet and silica probe were −46 and −70 mV, respectively. The zero of separation was calculated by fitting the weak forces at large separations (where deformation is insignificant) to the renormalized linear Poisson−Boltzmann eqs 6 and 7 on the basis of the predetermined ζ potentials.[18]

Results and Discussion

Interaction Forces and Deformation. Figure 1a shows a typical force versus piezo position plot for a silica sphere interacting with an immobilized, cross-linked PDMS droplet. The fact that the slope of the force versus position data is significantly less than the constant compliance slope (see line within Figure 1a), obtained for the silica colloid probe in contact with the glass substrate, is evidence of deformation. That is, upon approach of the cross-linked PDMS droplet to the silica probe, not all of the piezo-drive movement is transferred into cantilever deflection. The force data also show hysteresis; i.e., the force upon retraction is considerably less than on approach at the same piezo-drive position. Force curve hysteresis is evidence of a viscoelastic response and has been observed previously for polystyrene beads in air.[14] The time-dependent interactions and viscoelastic behavior of cross-linked PDMS droplets are discussed in the following section. Of further note, in Figure 1a there is evidence of a jump out-of-contact in the retraction force curve at a piezo position of ~120 nm. This phenomenon is indicative of a small adhesive force and is considered to be due to the stretching and then detachment of PDMS molecules bridged between the cross-linked droplet and the silica probe. Butt et al.[4] have observed similar effects due to the interaction of a cantilever tip with grafted polymers.

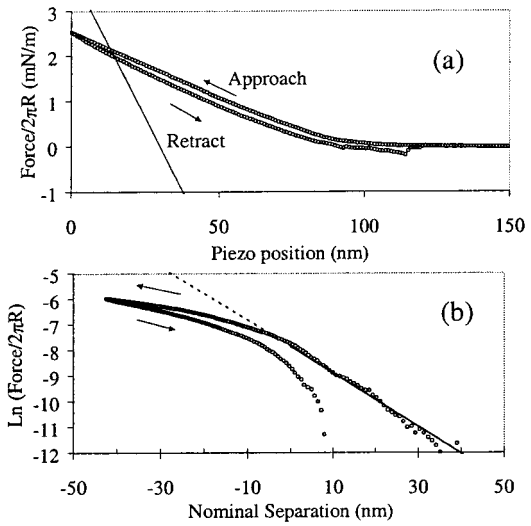

Figure 1. Force (determined by AFM) between a spherical silica probe ($R_1 = 3.5$ μm) and a cross-linked PDMS droplet (droplet A, $R_2 = 0.30$ μm) in 1 mM KNO_3 at pH 9.3, with an approach rate of 1 μm/s. (a) The piezo-position (arbitrary zero) is used for the abscissa. The solid line represents constant compliance for an equivalent rigid system. (b) The abscissa is the nominal separation, as determined from the renormalized linear Poisson−Boltzmann result for rigid spheres. The line is bold prior to zero and dashed past zero. The measured[19] ζ potentials of silica and PDMS (i.e. $\psi_1 = -70$ mV and $\psi_2 = -46$ mV) are used.

It should be recognized that plots of force against position are limited to only qualitative comparisons and it is more desirable to plot force data against actual separation. For nondeforming bodies, if the point of constant compliance can be ascertained, it is relatively trivial to convert piezo-drive position into the nominal separation between the bodies.[31] However, if one or both of the particles in an AFM force study are deformable, then the lack of rigid body compliance means that the zero of separation is not so readily determined. Only approximate methods have previously been reported for calculating the nominal separation between deformable colloids:

(i) Deformation is modeled as a Hookean spring, and the zero of separation is taken to be the point at which extrapolation of the linear compliance line reaches zero force.[10,11] This approach is only valid if the surfaces come into intimate contact in the constant compliance region. In the case of bubbles and droplets, often a liquid film remains between the surfaces and the zero is displaced by the thickness of the film.

(ii) Zero is assumed to be where deformed surfaces in contact have zero force.[32−34] Since this occurs due to the balance of van der Waal's attraction and steric repulsions, the amount of flattening can be substantial, and errors arise from ignoring it.

(iii) The zero of separation is taken to be the separation corresponding to the maximum force.[10,35,36] This approach also ignores the flattening of the deformable bodies and can be in serious error for compliant bodies.

(30) Cleveland, J. P.; Manne, S.; Bocek, D.; Hansma, P. K. *Rev. Sci. Instrum.* **1993**, *64*, 403.
(31) Ducker, W. A.; Senden, T. J.; Pashley, R. M. *Langmuir* **1992**, *8*, 1831.
(32) Weisenhorn, A.; Maivald, P.; Butt, H.-J.; Hansma, P. *Phys. Rev. B* **1992**, *45*, 11226.
(33) Snyder, B.; Aston, D.; Berg, J. *Langmuir* **1997**, *13*, 590.
(34) Burnham, N.; Colton, R. *J. Vac. Sci. Technol.* **1987**, *7*, 2906.
(35) Considine, R.; Hayes, R.; Horn. R. G. *Langmuir* **1999**, *15*, 1657.
(36) Schmitt, F.-J.; Ederth, T.; Weidenhammer, P.; Claesson. P.; Jacobasch, H.-J. *J. Adhes. Sci. Technol.* **1999**, *13*, 79.

(iv) The zero of separation is taken to occur at the point of the first measurable force.[12] This is appropriate for contact forces of zero range but is evidently incorrect for forces of extended range. A related method fixes the zero of relative separation at an arbitrary small force,[8] which allows comparison of data with the same force law but not if the forces are of different magnitude or type. For the case of van der Waal's forces, Burnham et al.[37] define contact as the position where a repulsion is first detectable, which they took to be signified by a change in curvature of the force.

(v) Mulvaney et al.[38] fit the nonlinear Poisson−Boltzmann equation for rigid bodies by adjusting both the zero of the experimental separation and the surface potential. This approach ignores deformation at small separations, which is where the linear and the nonlinear Poisson−Boltzmann equations differ, and at large separations an arbitrary change in surface potential can be compensated by a change in separation. In other words, one cannot determine unique values for the potential and the zero of separation simultaneously.

Recently, Gillies et al.[18] have developed a method to determine the zero of separation for AFM force measurements on deformable systems (bubbles, droplets, and deformable colloids). At large separations, the interaction forces are weak and no deformation is observed. Therefore, weak force data can be fitted to force laws of rigid body behavior. The nominal separation is determined by shifting this force data to the renormalized linear Poisson−Boltzmann eqs 6 and 7. This approach has been used for the data in Figure 1a, and the data are replotted against nominal separation in Figure 1b. All other force data in this article are analyzed in this way and plotted against nominal separation. Since nominal separation ignores deformation, when deformation does occur, the nominal separation differs from the actual separation and the behavior deviates from that of a rigid body. The extent of deformation and hysteresis can be observed more directly from Figure 1b. Negative nominal separations give the amount of flattening or deformation of the droplet. In Figure 1b it can be observed that approximately 40 nm of deformation has occurred. At this point, the measured force lies below the renormalized Poisson−Boltzmann prediction due to deformation of the PDMS. There is an initial deviation above the predicted rigid body behavior showing an increase in force. This initial deviation is most likely due to additional repulsive forces from a combination of steric and hydration interactions. The cross-linked PDMS droplets are composed of both linear and cyclic PDMS molecules,[29] which may lead to steric repulsion as observed for grafted polymers.[4] Hydration forces are known for silica surfaces[2] and may also occur between silica and PDMS surfaces. This steric contribution is small but we include it in the theoretical calculations below.

It should be recognized that the cross-linked PDMS droplets investigated in this study are prepared in a batch and those individual droplets may have different levels of cross-linking and hence different mechanical (nanorheological) properties. Our AFM investigations on different individual droplets have confirmed this variability. That is, from droplet to droplet there is a quantitative variation in the "deformability" and viscoelastic response. With this in mind, the force data presented below were collected from three different cross-linked PDMS droplets. The range of the forces observed,

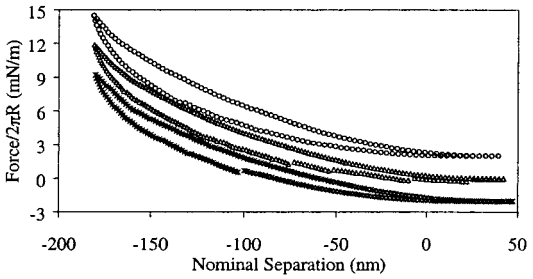

Figure 2. Force versus nominal separation plots for a spherical silica probe ($R_1 = 3.5\ \mu$m) and a cross-linked PDMS droplet (droplet B, $R_2 = 0.30\ \mu$m) in 1 mM KNO_3 at pH 9.3, at drive (approach and retraction) rates 0.6, 0.3, and 0.06 μm/s (plotted in descending order). For improved clarity, the 0.6 μm/s data have been shifted by 2 mN/m and the 0.06 μm/s data have been shifted by −2 mN/m.

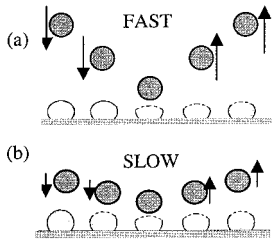

Figure 3. Schematic representation of the viscoelastic response of a cross-linked PDMS droplet during an approach−retraction AFM colloid probe investigation at (a) fast and (b) slow drive velocities.

and the extent of force curve hysteresis and adhesion, are clearly dependent on the droplet investigated as well as the experimental parameters, e.g. drive velocities and loading force.

Force Curve Hysteresis and Viscoelasticity. Figure 2 shows a series of force versus nominal separation plots for a cross-linked PDMS droplet and a silica probe determined at different drive velocities. For this particular droplet, at the applied loads investigated the level of adhesion was negligible. In general the level of adhesion between the silica sphere and PDMS droplets is considerably less than that reported between polystyrene spheres and mica surfaces in air.[14] We intend to report a more comprehensive investigation of deformation and adhesion of PDMS droplets. Here we note the stepping in the retract curves which indicate bridging of multiple tails. Here we concentrate on the time-dependent deformation behavior of the PDMS droplets. As the drive velocity is increased from 0.06 to 0.6 μm/s the maximum force measured increased from 11.2 to 12.5 mN/m. This reflects the fact that at a greater approach rate there is less time for deformation and flattening to occur and the cross-linked droplet appears stiffer.

The viscoelastic response of a cross-linked PDMS droplet is further demonstrated by the approach-rate-dependent force curve hysteresis shown in Figure 2. Upon deformation of a viscoelastic body a characteristic time is required to relax back to its original position. Force curve hysteresis is observed when the time required for the deformed colloid to relax is comparable to the time for retraction; this is shown schematically in Figure 3. Under these conditions, at a given nominal separation the actual separation on retraction will be greater than on approach. At infinitely slow drive velocities (loading and unloading) negligible force curve hysteresis would be expected.[20,28] It is clear from Figure 2 that for drive velocities in the range 0.06 to 0.6 μm/s the time for droplet relaxation is comparable to the time scale of the loading/unloading cycle and

(37) Burnham, N. A.; Colton, R. J.; Pollock, H. M. *Nanotechnology* **1993**, *4*, 64.

(38) Mulvaney, P.; Perera, J.; Biggs, S.; Grieser, F.; Stevens, G. *J. Colloid Interface Sci.* **1996**, *183*, 614.

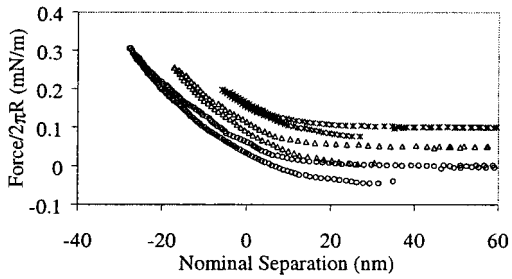

Figure 4. Force versus nominal separation plots for a spherical silica probe ($R_1 = 3.5\ \mu$m) and a cross-linked PDMS droplet (droplet C, $R_2 = 0.30\ \mu$m) in 1 mM KNO_3 at pH 9.3, at a drive rate of 1 μm/s, at different maximum applied loads 0.1, 0.2, and 0.3 mN/m (from right to left). For improved clarity, the 0.1 mN/m data have been shifted by 0.1 mN/m and the 0.2 mN/m data have been shifted by 0.05 mN/m.

significant hysteresis is observed. Upon approach the viscous component of the cross-linked PDMS droplet leads to energy dissipation and the elastic component leads to energy storage. The energy dissipation is reflected in the area inside the hysteresis loop of the force versus nominal separation data. At faster drive velocities more energy is stored elastically. On the subsequent retraction there is more energy dissipated to viscous effects than at lower velocities. Consequently, viscous dissipation of the energy and the area within the hysteresis loop increases. In the case of Figure 2 we find the energy dissipated is 5.5×10^{-17} J at 0.06 μm/s, 6.6×10^{-17} J at 0.3 μm/s, and 7.5×10^{-17} J at 0.6 μm/s.

In further exploring the viscoelastic response of the cross-linked PDMS droplet, we consider the influence of the maximum applied load on force versus nominal separation plots (Figure 4). Variation in applied load was achieved at constant drive amplitude by altering the point at which the piezo crystal starts the drive. In this manner the approach rate remains constant, which would not be the case if the drive amplitude was varied instead. That is, the influence of the applied load is investigated without changing the approach rate. The maximum applied load was varied from 0.1 to 0.3 mN/m. In all cases, the force plots show hysteresis, and this increases with increasing applied load and hence deformation. These findings confirm the viscoelastic nature of the cross-linked droplets. It is interesting to note that although the applied loads employed in Figure 4 were less than those employed in Figures 1 and 2 (i.e. a weaker cantilever was used), there is still evidence for weak adhesion. Adhesion would generally be expected to be more strongly dependent on the loading force. In the present system adhesion is considered insignificant, but there is some variation from droplet to droplet due to differences in their structure.

Application of Viscoelastic Theory: Determination of Nano-rheological Properties. A theoretical approach for describing the viscoelastic deformation of spheres[20] was described earlier in this article and has been employed to extract the nanorheological properties of cross-linked PDMS droplets. Theoretical fits to the force versus separation data at different approach rates and applied loads are given in Figures 5 and 6, respectively. The values for E_0, E_∞, and τ were determined to be 1.2×10^6 N m^{-2}, 0.8×10^6 N m^{-2}, and 0.07 s, respectively. These values for elastic parameters agree well with the value of 0.6 MPa measured by Geniesser et al.[39] for cross-linked PDMS using a lateral force rheometer. Genieser et al. also found that the loss modulus became significant at

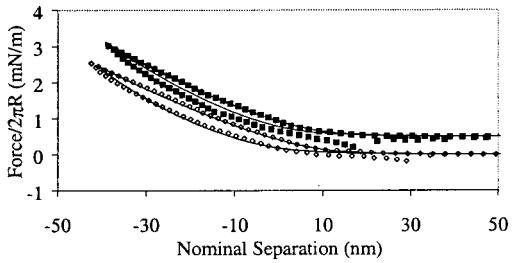

Figure 5. Force versus nominal separation plots for a spherical silica probe ($R_1 = 3.5\ \mu$m) and a cross-linked PDMS droplet (droplet A, $R_2 = 0.30\ \mu$m) in 1 mM KNO_3 at pH 9.3, at drive rates of 1 μm/s (◇) and 4 μm/s (■). The lines are theoretical fits to the data, where $E_0 = 1.2$ MPa, $E_\infty = 0.8$ Mpa, and $\tau = 0.07$ s, for equivalent approach rates. For clarity the 4 μm/s data have been shifted by 0.5 mN/m.

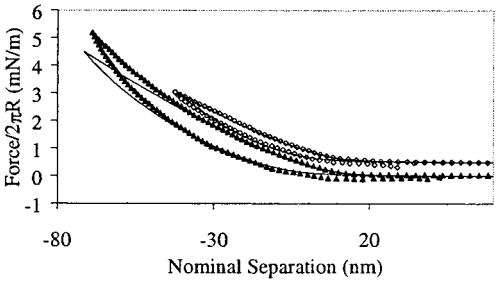

Figure 6. Force versus nominal separation plots for a spherical silica probe ($R_1 = 3.5\ \mu$m) and a cross-linked PDMS droplet (droplet A, $R_2 = 0.30\ \mu$m) in 1 mM KNO_3 at pH 9.3, at a drive rate of 1 μm/s, at different applied loads 2.5 mN/m (◇) and 5.2 mN/m (▲). The curved lines are theoretical fits to the data, using the parameters from Figure 5. For clarity the 2.5 mN/m data have been shifted by 0.5 mN/m.

about 3 Hz, which implies a time scale of the same order as the 0.07 s relaxation time that we measure. Obviously these values are highly dependent on composition and degree of cross-linking of the PDMS. Nevertheless the agreement with literature values is encouraging. It is also encouraging that, in agreement with the experimental observations, the viscoelastic theory predicts force curve hysteresis, whereas traditional elastic theories do not. The theory also predicts the approach rate and loading force dependency of the force curve hysteresis. Figure 6 shows excellent agreement between experimental and theory at low loading forces, but as the loading force and deformation is increased the theory underestimates the experimentally determined force data, even though it adequately predicts the amount of force curve hysteresis. This deviation from theory is considered to be due to a combination of two effects: At relatively large deformations, we begin see an influence of the rigid substrate underneath the droplet. It is also likely there is a contribution from the structure of the cross-linked PDMS droplet. That is, it is likely there exists a greater cross-linking density in the center of the droplet, as has been seen in thin films studied by neutron reflectometry.[40] Hence, the nanorheological response may not be completely described by one set of elastic and viscous moduli. This chemical and physical variability of the droplets may also lead to differences in the level of polymer bridging and adhesiveness; these are not accounted for by the viscoelastic theory. The fitted parameters represent an average value of the entire droplet.

(39) Genieser, L. H.; Hendriks, K. C. P.; Baaijens, F. T. P.; Meijer, H. E. H. *J. Rheol.* **2000**, *44*, 1003.

(40) Yim, H.; Kent, M.; McNamara, W. F.; Ivkov, R.; Satija, S.; Majewski, J. *Macromolecules* **1999**, *32*, 7932.

Summary and Conclusion

Colloid probe AFM has been used to determine the deformation and nanorheological properties of a cross-linked PDMS droplet immobilized on a flat substrate. On approach of the surfaces, as a result of deformation of the PDMS the repulsive force increases much less rapidly than expected for the electrical double layer interaction of rigid particles. The zero of separation may be determined by comparing the experimental force data with that predicted due to overlapping double layers at large separations where deformation is negligible. On retraction of the surfaces, force curve hysteresis is observed due to the viscoelastic response of the PDMS droplet. By comparison with viscoelastic theory, the moduli (viscous and elastic) and the characteristic relaxation time of the PDMS colloid have been determined. It is concluded that quantitative analysis of AFM force measurements with viscoelastic theory offers a viable method to determine the nanorheological properties of soft colloid particles.

Acknowledgment. The Australian Research Council's Special Research Centre for Particle and Material Interfaces is acknowledged for funding this work.

LA011461G